Korean J. Chem. Eng., 38(8), 1660-1668 (2021)
DOI: 10.1007/s11814-021-0808-2

pISSN: 0256-1115
eISSN: 1975-7220

Synergistic effect of sono-photocatalytic processes on sludge disintegration

Asaad Olabi and Sayiter Yildiz†

Sivas Cumhuriyet University, Engineering Faculty, Department of Environmental Engineering, 58140, Sivas, Turkey
(*Received 14 February 2021 • Revised 10 April 2021 • Accepted 11 April 2021*)

Abstract−The synergistic effect of the combination of sono-photocatalytic oxidation and Fenton reagents was investigated on sewage sludge disintegration. In this context, the simultaneous effect of ultrasound (US) and UV irradiation was studied with variable parameters such as the duration of photocatalysis, catalyst amount and different UV light. The optimum amount of TiO_2 and Fenton reagent determined in the sono-photocatalytic process was kept constant. Different combinations of advanced oxidation processes (AOPs) showed different degree of disintegration (DD). While H_2O_2 added to sono-photocatalytic application with TiO_2 contributed to the increase of DD, iron addition caused a decrease in DD. This decrease was more in Fe^{2+} use than Fe^0. DD was determined as 18.35%, 20.60% and 32.58% in TiO_2/UVA, TiO_2/H_2O_2/UVA, and TiO_2/H_2O_2/UVA/US processes, respectively. In TiO_2/UVB process DD was found to be 17.60%, while it reached 30.34% in TiO_2/UVB/US, 43.82% in TiO_2/CFP/UVB/US and 52.81% in TiO_2/MFP/UVB/US. In the kinetic study, it was determined that all processes comply with zeroth order kinetics. The use of ultrasound in all processes increased the germination percentage, which expresses the toxicity of the sludge, up to 100%. After sono-photocatalytic disintegration, the sludge volume decreased by 19.2% to 60% according to values of volume-weighted average. It was concluded that the sono-photocatalytic process has an important effect on sludge disintegration, which is an effective method for sludge minimization. In addition, it was determined that the synergistic effect of fenton reagents added to the process was strong and the combined use of these two processes increased the DD value from 17.60% to 52.81%.

Keywords: Sludge Disintegration, Ultrasonic, Photocatalysis, TiO_2, Fenton, UV

INTRODUCTION

Increasing attention has been paid to minimizing the amount of sewage sludge in the waste water treatment process. Research on sludge treatment is increasing daily and some new sludge reduction techniques are being suggested [1-3]. One such reduction technique is sludge disintegration. Sludge disintegration can be achieved by degradation of the bacterial flora or microorganism cells in the sludge depending on the type and the intensity of disintegration [4].

Advanced oxidation processes (AOPs) are one of the best methods for the degradation and mineralization of organic matter as well as increasing biodegradability [5]. The use of AOPs for the disintegration of sewage sludge, which has the advantage of rapid oxidation of pollutants to harmless end products, has increased. Many AOPs and innovative disintegration processes have been investigated for the disintegration and reduction of sludge. The application of heterogeneous photo-catalysis processes using semiconductors, such as TiO_2 and ZnO, and UV in sludge treatment is drawing attention [6-8]. TiO_2 nanoparticles are efficient photocatalysts due to their favorable bandwidth, large surface area and non-toxicity [9]. The photocatalytic properties are derived from the formation of photogenerated charge carriers (gaps and electron) which takes place upon absorption of UV light conformable to the band-gap. The photogenerated gaps in the valence band form hydroxyl radicals (•OH) due to diffusion to the TiO_2 surface and reaction with adsorbed water molecules [10,11].

Fenton reagent is a mixture of hydrogen peroxide and iron salts, an effective oxidant for a wide variety of organic compounds. During the decomposition of hydrogen peroxide catalyzed by iron salts, •OH radicals are formed [12].

$$Fe^{2+}+H_2O_2 \rightarrow Fe^{3+}+\bullet OH+OH^- \quad (1)$$

A disadvantage of this method is that when divalent iron becomes trivalent, the oxidative activity of the Fe^{2+}/H_2O_2 system is significantly reduced. The result of this situation is that significant amounts of the above reagents are consumed, as well as large amounts of sludge being formed from iron sedimentation. If trivalent iron is converted back into bivalent by light radiation (UV), the efficiency and yield of the method can be significantly increased. The amount of •OH that increases with the UV effect enhances the yield [13].

$$Fe^{3+}+H_2O+h\upsilon\,(\lambda<450\text{ nm}) \rightarrow Fe^{2+}+\bullet OH+H^+ \quad (2)$$

This method contributes to the regeneration of radicals in several basic steps of the reaction mechanism. Moreover, hydrogen peroxide can generate two hydroxyl radicals initiated by UV light, according to the following reaction [14]:

$$H_2O_2+h\upsilon \rightarrow 2\bullet OH \quad (3)$$

The Sono-Photo Fenton process requires a low amount of iron salt compared to the Fenton. This is of great economic importance. Sono-Photo Fenton can be explained by Eqs. (4)-(8) [15].

†To whom correspondence should be addressed.
E-mail: sayiteryildiz@gmail.com

$$Fe^{3+}+H_2O+h\upsilon \rightarrow Fe^{2+}+\bullet OH+H+ \quad (4)$$

$$\bullet OH+HO\bullet_2 \rightarrow H_2O+O_2 \quad (5)$$

$$HO\bullet_2+HO\bullet_2 \rightarrow H_2O_2+O_2 \quad (6)$$

By US,

$$H\bullet+H_2O_2 \rightarrow \bullet OH+H_2O \quad (7)$$

$$Fe^{3+}+H\bullet \rightarrow Fe^{2+}+H^+ \quad (8)$$

Alternative processes include the use of photocatalysts as ultrasound or nano-sized TiO_2 with UV radiation in the oxidation of organic matter due to non-toxicity, stability of the chemical structure, electrical and optical properties [16]. Photocatalysis efficiency can be improved using high or low frequency due to the effects of the chemical and physical properties of ultrasound on the regeneration of the catalyst surface and the formation of free radicals [17]. When TiO_2 photocatalysts are irradiated by the US, organic molecules are oxidized both by excitation of electrons in the TiO_2 band gap [18] and by ultrasonic separation of water molecules according to the following equations (Eqs. (9)-(12)) [19].

$$TiO_2+h\upsilon \rightarrow TiO_2(e^-)+TiO_2(h^+) \quad (9)$$

$$h^++OH^-_{ads} \rightarrow \bullet OH \quad (10)$$

$$e^-+O_2 \rightarrow O_2^- \rightarrow \bullet OH \quad (11)$$

$$H_2O+))) \rightarrow H\bullet+\bullet OH \quad (12)$$

$$\bullet OH+\bullet OH \rightarrow H_2O_2 \quad (13)$$

Combinations of Fenton reaction and photocatalysis have been reported by many groups [20-22]. In addition, the combination of photocatalytic and ultrasounds [23,24], ultrasound and Fenton reaction, and three techniques [25] has been used in different studies. Also, the hydrodynamic cavitation method has been used in WAS applications recently [26-28].

Ultrasonic frequencies range from 20 kHz to 100 MHz. US frequently used in sludge disintegration is at a frequency of 20-50 kHz [29,30]. US can be used with other methods as a combined process. Lu et al. [31] have shown that the combined alkaline-ultrasound process increased solubility in the sludge by producing low molecular weight substances. Kim et al. [32] applied ultrasonic treatment to sludge pre-treated with alkali. The increase in SCOD/TCOD was limited to 50% in individual pre-treatment, while it reached 70% in combined pre-treatment. Wang et al. [33] investigated a photosynthetic bioelectrochemical system combined with ultrasonic treatment to mineralize sludge. Man et al. [34] examined the removal of polycyclic aromatic hydrocarbons (PAH) from textile dyeing sludge with a combined US and zero-valence iron/EDTA/Air (ZEA) system. Gong et al. [35] focused on the effects of combined US and Fenton oxidation (US+F) on disintegration of treatment sludge in pre-treatment processes.

There is no published study investigating the synergistic effects of sono-photocatalytic process and Fenton reagents on sludge disintegration. In this study, unlike other sludge disintegration methods, disintegration of the sludge under different UV lights was investigated in a reactor where both the photocatalytic oxidation process (FOP) (UV+TiO_2) and combined processes (TiO_2/iron, TiO_2/H_2O_2 and TiO_2/iron/H_2O_2) were used together with ultrasonic process. In addition to DD calculation, toxicity, particle size distribution and kinetic studies were carried out for each process. Especially, this study is an important and first in terms of revealing the synergistic effect of these processes in an integrated reactor. Experiments were performed three times and the mean values of the samples presented. The data presented are mean values from experiments, standard deviation (3%) and error bars are indicated in the figures.

MATERIALS AND METHODS

In the study, SCOD was chosen as the target parameter. Thus, process optimizations, kinetic study and disintegration degree (DD) calculation were performed based on the SCOD parameter. UV-A (365 nm), UV-B (302 nm), and UV-C (256 nm) lights were used as UV source. The study was carried out in three experiment sets. The first set is the determination of optimum reagent doses in sludge disintegration by applying different doses of fenton reagents and TiO_2 semiconductor (I). While determining the reactive amount ranges, the amounts used in previous studies on sludge disintegration with Fenton were taken into account [36,37]. The next experiments involved the optimum Fenton reagents with the simultaneous use of UV irradiation (II). Finally, more simultaneous disintegration effect was achieved with three methods by applying ultrasound at 40 kHz frequency and 180 watt power (III). Sono photocatalytic experiments were carried out in a custom-built reactor (Fig. 1). Moreover, toxicity analyzes and particle size analysis were performed for raw sludge and disintegrated sludge to observe the effect of disintegration on particle degradation of the sludge.

Waste activated sludge used in this study (WAS) was taken from the recycle line of sewage treatment plant (activated sludge process) at Sivas/Turkey. The samples were promptly brought to the laboratory and stored into a refrigerator at +4 °C. Raw sludge has characteristics such as pH 6.5, SCOD 40 mg/L, total COD 9,800 mg/L, total solids (TS) 8,285 mg/L, suspended solid (SS) 5,950 mg/L, electrical conductivity (EC) 1,040 μS/cm, and a TS content of 1%.

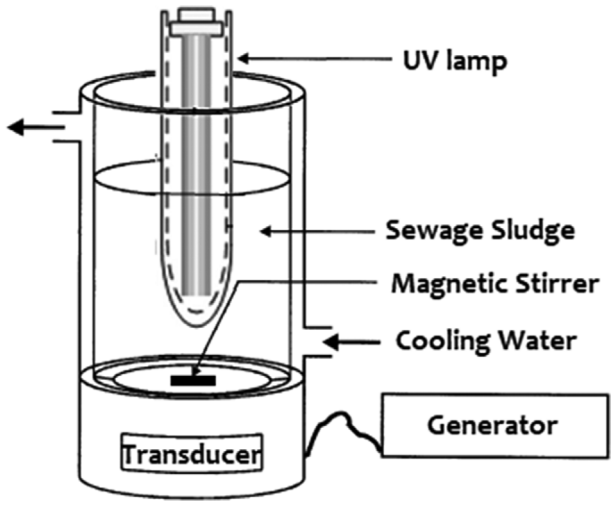

Fig. 1. Schematic view of sono-photo-Fenton application reactor.

COD, SCOD and SS analyses were performed according to standard methods (Standard Methods Committee, 1997). A multi-parameter device (Thermo Orion - STARA2145) was used for pH and EC measurements. Particle size distribution analyses were conducted with a Malvern Mastersizer 2000QM brand particle size analyzer.

The zero-valent iron (Fe^0) used for the modified Fenton process (MFP) in the study was prepared in the laboratory. Therefore, a solution of 1 M $NaBH_4$ (3.05 g $NaBH_4$ soluble in 100 mL of distilled water) was added dropwise, while 5.34 g $FeCl_2{\cdot}4H_2O$ was stirred in 30 mL solution (24 mL ethanol+6 mL distilled water) on magnetic stirrer. After the $NaBH_4$ was added completely, it was mixed in the mixer for another 10 minutes. The resulting black mud was separated by centrifugation, washed with 25 mL ethanol, then centrifuged again and dried at 50 °C until completely dry [38].

Classical Fenton process (CFP) experiments were carried out using a stock solution of $FeSO_4{\cdot}7H_2O$ and 35% H_2O_2 as Fenton reagent. The experiments were cconducted in 250 ml glass beakers for raw sludge sample in 250 ml liquid volume. MFP experiments were carried out in the procedure followed in CFP. But, instead of ferrous iron, metallic iron powder (Fe^0) was used. Experimental conditions are given in Table 1.

Table 1. Experimental conditions

Experiment code	Description
CFP and MFP	Fe^{2+} and Fe^0 optimization; The reaction time was 60 min, pH 3, H_2O_2 35 g/kg TS was kept constant and the iron concentration was examined in the range of 1-50 g/kg TS. The optimum dose was 7 g/kg TS for Fe^{2+} and 5 g/kg TS for Fe^0 (Fig. 2(a)). H_2O_2 optimization; By keeping the optimum iron doses constant, H_2O_2 was examined in the range of 1-100 g/kg TS, and optimum H_2O_2 concentrations were determined as 35 g/kg TS for Fe^{2+} and 25 g/kg TS for Fe^0 (Fig. 2(b)).
Photocatalytic oxidation	Oxidation was performed by applying different amounts of TiO_2 (0.05-1.4 g/l) using pH 3, time 60 minutes and UV-A light. The optimum TiO_2 amount was determined to be 0.7 g/l (Fig. 2(c)).
pH effect	To determine the pH effect, the pH was changed in the range of 2-9 with constant parameters: TiO_2 0.7 g/l, time 60 min, and in the presence of UV-A. The optimum pH was determined as 3 (Fig. 2(d)).

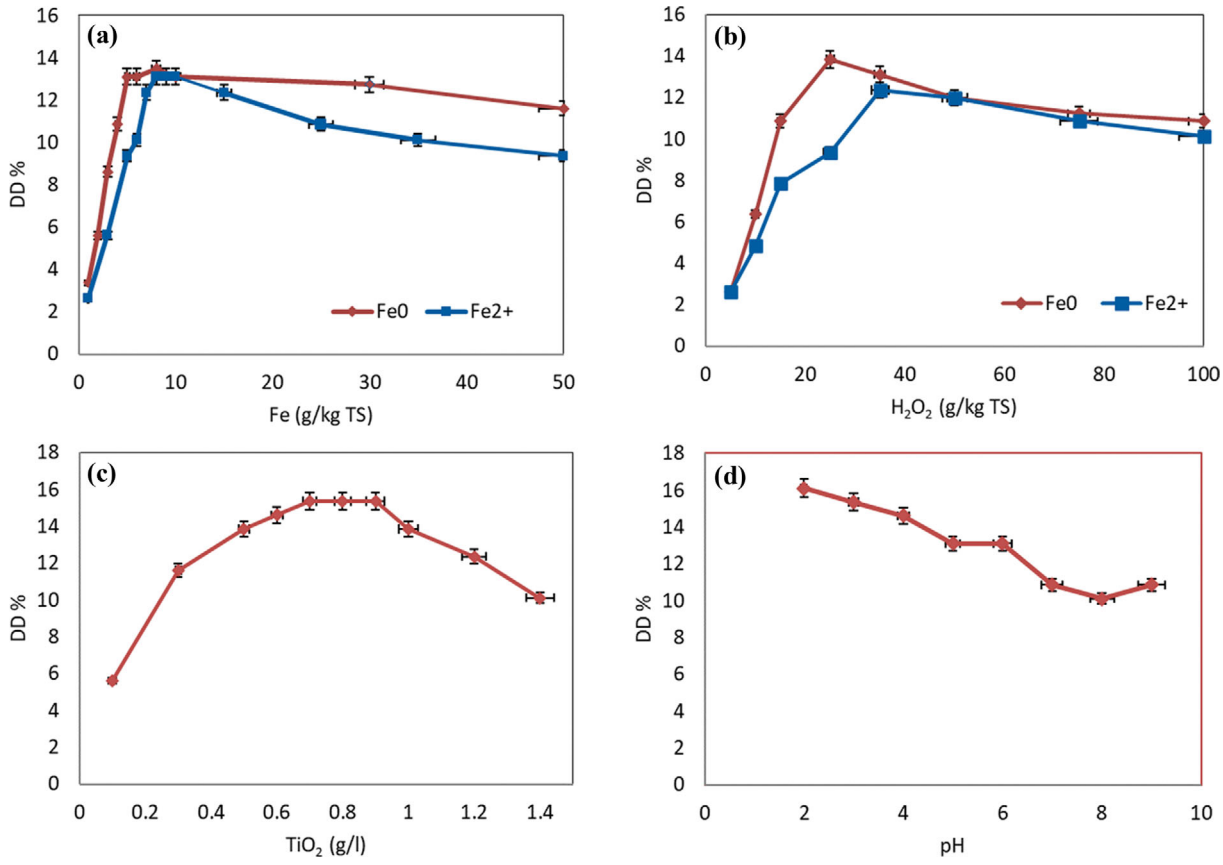

Fig. 2. DD changes depending on the Fe (a), H_2O_2 (b), TiO_2 (c) dose and pH (d).

To evaluate the sludge disintegration performance, DD was calculated using Eq. (14) [39];

$$DD_{COD} = \frac{(SCOD - SCOD_0)}{SCOD_{NaOH} - SCOD_0} * 100 \quad (14)$$

Here, SCOD soluble COD value (mg/L) of the disintegrated sludge (mg/L), $SCOD_0$ soluble COD value (mg/L) of the non-disintegrated sludge (raw sludge), $SCOD_{NaOH}$ soluble COD value (mg/L) of sludge disintegrated chemically with 1 mol/L NaOH at room temperature, 20±1 °C over 24 hours.

The toxicity effects of different disintegration applications were also determined. In this context, the seed germination test, which indicates toxicity, was performed for raw and disintegrated sludge. The appearance of radicals in the petri dish indicates seed germination [40]. Sludge samples were filtered by vacuum filtration. 10 mL of filtrate was transported to Petri dish and incubated at 28 °C after placing ten spinach seeds (Spinacia oleracea) in each Petri dish. The experiment was conducted for ten days. The seeds from which radicals began to emerge (germinated) were counted. The percentage of germination (GP) was calculated using Eq. (15) [41].

$$GP = \frac{\text{Number of seeds germinated}}{\text{Number of seeds planted}} * 100 \quad (15)$$

RESULTS AND DISCUSSION

1. Determination of Reaction Time

The study was carried out using the optimum doses (Table 1) to determine the reaction time for each of TiO_2/UV (FOP), Fe^{2+}/H_2O_2/UV (CFP) and Fe^0/H_2O_2/UV (MFP) processes. The change of SCOD and DD depending on time in the 0-120 min interval was determined at room temperature (Fig. 3). The long or short reaction time is related to the degradation ability of organic substances in the sludge structure. The short time required for decomposition references that the sludge contains easily degradable organic substances. The long time indicates the presence of hardly degradable organic substances [42].

As can be seen in Fig. 3, the oxidation reaction occurred rapidly in the use of Fe^{2+} because the catalyst iron and H_2O_2 were present in adequate amount in the reaction medium in the first 5 minutes, while it was more slowly in the use of Fe^0 because it relies on the dissolution of metallic iron. A similar situation is valid for the use of TiO_2. In all three processes, as a result of the decrease of reaction components in the medium over time, the rate of the increase in SCOD slows. Accordingly, it was determined that the disintegration of the sewage sludge was realized in two stages: the fast oxidation stage in the first 30 minutes and the slow oxidation stage in the remaining 30 minutes. There was no significant change after 60 minutes. The optimum time in this study was determined as 60 minutes.

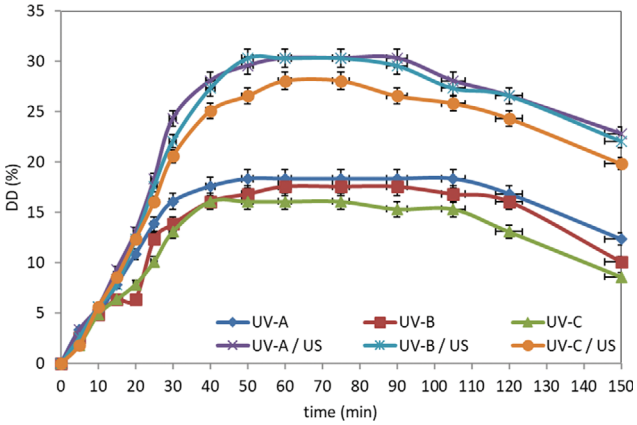

Fig. 4. DD changes depending on the reaction time for photocatalytic and sono photocatalytic reactions (Experimental conditions: pH 3, 0.7 g/l TiO_2).

2. Sono-photocatalytic Effect

Using the TiO_2 amount obtained in the optimization study, photocatalytic and sono-photocatalytic processes were carried out under different UV lights for 0-150 minutes. The results obtained are given in Fig. 4.

As seen in Fig. 4, DD increased rapidly in the first 30 minutes in all processes. Then the increase slowed and became constant after

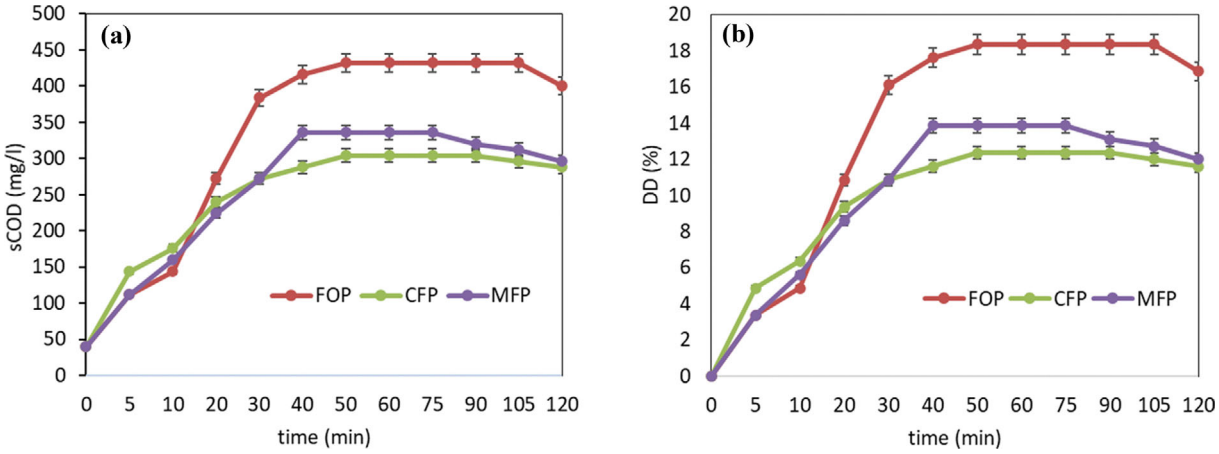

Fig. 3. SCOD (a) and DD (b) changes depending on the reaction time for different applications (Experimental conditions: pH 3, 7 g/kg TS Fe^{2+}/35 g/kg TS H_2O_2 and 5 g/kg TS Fe^0/25 g/kg TS H_2O_2).

Table 2. Kinetic constants

	Zero-order model		First-order model		Second-order model	
	k_0 (mg/L·min)	R^2	k_1 (1/min)	R^2	k_2 (L/mg·min)	R^2
TiO_2/UV-A	6.8688	0.87	0.033	0.7	−0.0002	0.44
TiO_2/UV-B	6.6361	0.91	0.0337	0.77	−0.0002	0.49
TiO_2/UV-C	6.2353	0.91	0.0334	0.76	−0.0003	0.51
TiO_2/UV-A/US	12.011	0.93	0.0418	0.77	−0.0002	0.45
TiO_2/UV-B/US	12.214	0.95	0.0432	0.8	−0.0003	0.49
TiO_2/UV-C/US	10.981	0.95	0.0421	0.78	−0.0003	0.5

50 minutes. After the 90th minute, DD showed a decreasing trend. The highest DD values of 30.34% were obtained in TiO_2/UV-A/US and TiO_2/UV-B/US sono-photocatalytic processes. In the photocatalytic process, DD was 18.35% and 17.6% when TiO_2/UV-A and TiO_2/UV-B were applied, respectively. Mineralization of dissolved organic substances by photocatalytic reaction may be dominant after the 90th minute. In the first 50 minutes, the amount of COD solubilized by the photocatalysis reaction was superior to that of dissolved organic substances mineralized by the photocatalysis reaction. Also, the mineralization rate after 90th minutes is faster than the solubilization rate. In this study, the optimum time was determined as 60 minutes. Since ultrasound in the sono-photocatalytic process causes the solid phase to dissolve [43], the sludge disintegration efficiency increased.

3. Kinetic Study

Zero (Eq. (16)), first (Eq. (17)) and second-order (Eq. (18)) kinetic models were applied to the changing SCOD concentrations depending on time of sono-photocatalytic and photocatalytic oxidation processes [44]. Kinetic parameters calculated for reaction kinetics are given in Table 2.

$$C = C_0 - k_0 \cdot t \tag{16}$$

$$\ln C = \ln C_0 - k_1 \cdot t \tag{17}$$

$$\frac{1}{C} = \frac{1}{C_0} + k_2 \cdot t \tag{18}$$

Here, C_0 initial SCOD concentration (mg/L); C SCOD concentration at any time (mg/L); k_0, k_1 and k_2 kinetic constants of zeroth, first and second order reaction kinetics, respectively; and t represents the reaction time (minutes).

As seen in Table 2, each application of FOP conforms to the zeroth order kinetics as a function of the SCOD concentration. Similar results have been found in different studies [44,45]. It was observed that the k_0 value increases when US is used; the k_0 value increased from 6.6361 to 12.214 in the TiO_2/UV-B/US process. This increase can be explained by the relative increase in temperature due to energy released from ultrasound [46].

4. Effect of Iron Catalyst on Sono-photocatalytic Process

The effect of the combination of TiO_2 and iron on sono-photocatalytic disintegration in different UV lamps was investigated under the optimum conditions previously determined (Table 1). DD values calculated for each process are given in Fig. 5.

As seen in Fig. 5, the highest DD occurred in sono-photocatalytic processes without iron addition. While the DD was 30.34% for UVA and UVB, it was calculated as 28.09% for UVC. The iron catalyst added to the process reduced the disintegration efficiency. This decrease was slightly higher in Fe^{2+} usage than in Fe^0 usage. When Fe or other metals are added to TiO_2, the superficial complexing properties may change. The formation of superficial complexes in photochemical reactions can exhibit charge transfer ab-

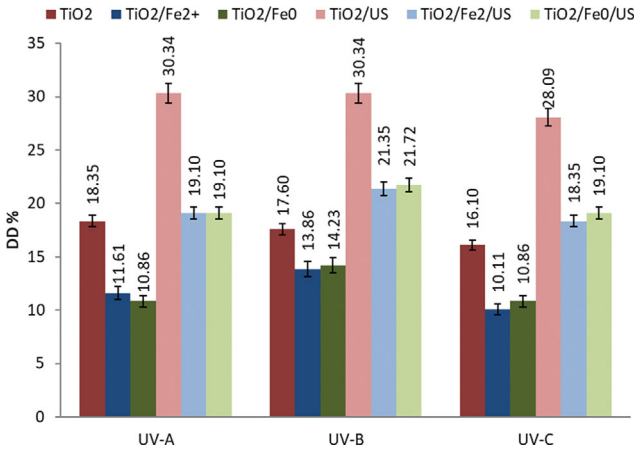

Fig. 5. DD values for sono-photocatalytic and iron combined processes (Experimental conditions: pH 3, 7 g/kg TS Fe^{2+}, 5 g/kg TS Fe^0, 0.7 g/l TiO_2 and time 60 mimutes).

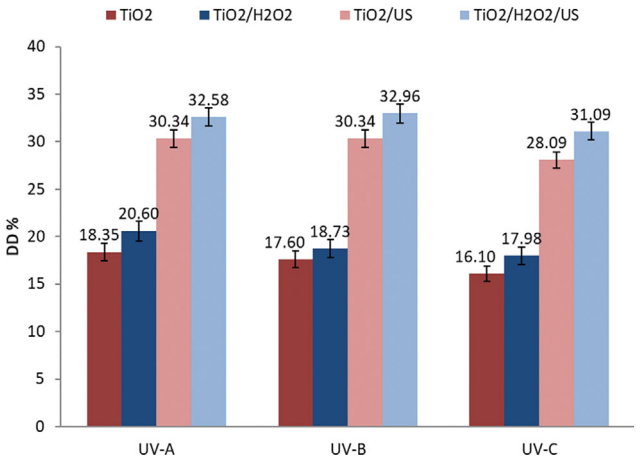

Fig. 6. DD values for sono-photocatalytic and H_2O_2 combined processes (Experimental conditions: pH 3, 0.7 g/l TiO_2, 35 g/kg TS H_2O_2 and time 60 mimutes).

Table 3. Operation cost for considered processes

	Iron catalyst cost ($)	H_2O_2 cost ($)	TiO_2 cost ($)	UV energy cost ($)	US energy cost ($)	Total operation cost ($)
CFP/TiO_2/UV	2.6×10^{-4}	1.0×10^{-3}	2.6×10^{-3}	7.2×10^{-4}	-	4.58×10^{-3}
MFP/TiO_2/UV	3.6×10^{-3}	7.0×10^{-4}	2.6×10^{-3}	7.2×10^{-4}	-	7.62×10^{-3}
CFP/TiO_2/UV/US	2.6×10^{-4}	1.0×10^{-3}	2.6×10^{-3}	7.2×10^{-4}	8.7×10^{-3}	13.28×10^{-3}
MFP/TiO_2/UV/US	3.6×10^{-3}	7.0×10^{-4}	2.6×10^{-3}	7.2×10^{-4}	8.7×10^{-3}	16.32×10^{-3}

sorption bands at intervals similar to those corresponding to homogeneous complexes and similar photolytic behavior [47]. Fe reduces the gap band of TiO_2 and leads to increased active sites on its surface [48].

5. Effect of H_2O_2 on Sono-photocatalytic Process

The effect of H_2O_2 added to the sono-photocatalytic process on disintegration under different UV lamps was investigated by using optimum TiO_2 and H_2O_2 (Table 1). DD values obtained are shown in Fig. 6.

Unlike iron catalyst, the addition of H_2O_2 to the sono-photocatalytic process had an efficiency enhancing effect. While the DD was 30.34% in the sono-photocatalytic process conducted with UVA and UVB light, it increased to 32.58% and 32.96%, respectively, with the addition of H_2O_2. As a result of photolysis of H_2O_2 by UV light, additional •OH was produced and thus contributed to the increase of disintegration efficiency [49]. The catalytic activity is significantly increased in the presence of UV light, US irradiation and H_2O_2 [50].

6. Synergistic Effect of Sono-photocatalytic Process and Fenton Process (Fe/H_2O_2)

The synergistic effects on sludge disintegration were investigated by using the sono-photocatalytic process and fenton reagents together. The amount of reagents used are the optimum values given in Table 1. DD values obtained are given in Fig. 7.

As shown in Fig. 7, the combined use of Fenton and sono-photocatalytic process significantly increased disintegration. The highest DD value occurred under UVB light. In addition, the synergistic effect realized with MFP is higher than other processes. The DD obtained by the combination of the sono-photocatalytic process and MFP was 52.81%, while it was calculated as 43.82% in the sono-photocatalytic-CFP combined process. The DD values obtained by using the MFP or CFP together with the photocatalytic process performed without ultrasound were determined as 33.33% and 28.84%, respectively. In the study, it was revealed that Fenton reagents used with the sono-photocatalytic process have a highly effective synergistic effect on sludge disintegration.

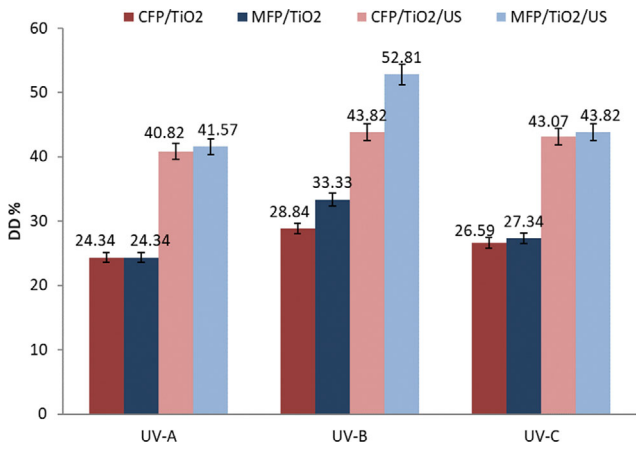

Fig. 7. DD values for sono-photocatalytic and Fenton combined processes (Experimental conditions: pH 3, 7 g/kg TS Fe^{2+}/35 g/kg TS H_2O_2, 5 g/kg TS Fe^0/25 g/kg TS H_2O_2, 0.7 g/l TiO_2 and time 60 mimutes).

7. Economic Evaluation

In the study, economic evaluations of the synergistic effects on sludge disintegration were made (Table 3). The operating costs of the processes were calculated by considering the amount of reagents ($FeSO_4{\cdot}7H_2O$, Fe^0, H_2O_2 and, TiO_2) as well as UV and US energy costs. In the calculation, optimum conditions were taken into account. It was assumed that the cost of H_2O_2 was 5.5 $/kg, the cost of $FeSO_4{\cdot}7H_2O$ was 3.65 $/kg, the cost of Fe^0 was 0.35 $/g and the cost of TiO_2 14.9 $/kg. Fe^0 cost was obtained by calculating. Electricity price (kWh) was 0.048 $. Reaction time is 60 minutes for UV and US. Also, Fig. 8 displays the overall costs as a percentage of the most expensive disintegration.

When carrying out the disintegration without US, the estimated relative cost decreased in a 53 and 72%, respectively, being the MFP/TiO_2/UV and CFP/TiO_2/UV the cheaper option. However, the highest DD values belong to synergistic processes using US.

8. Toxicity Analysis

The seed germination test expressing toxicity was carried out for raw and disintegrated sludge with the highest DD obtained from

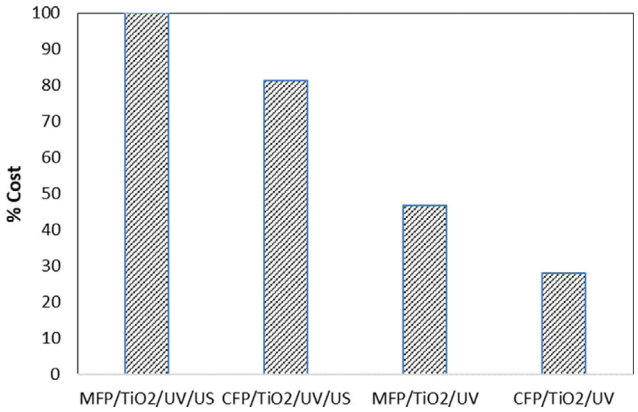

Fig. 8. Relative economic cost per functional unit for considered processes.

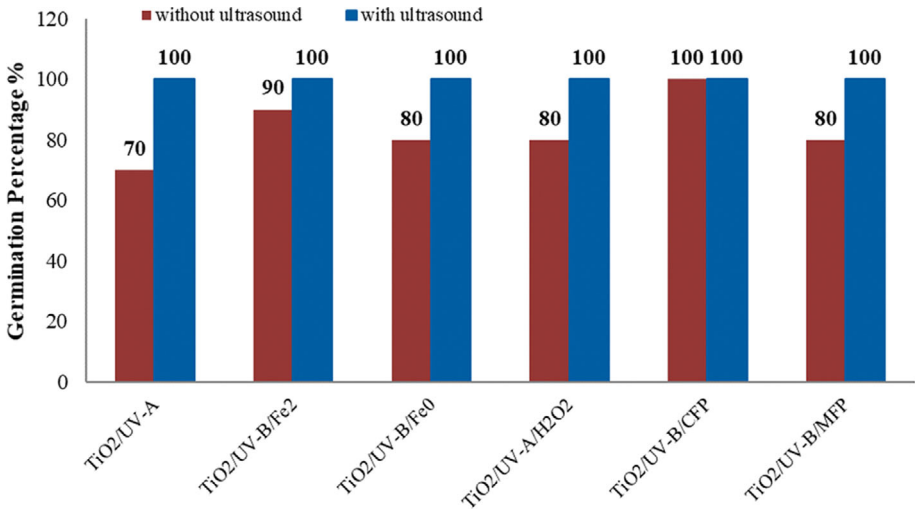

Fig. 9. Percentage of germination within the scope of toxicity analysis after processes.

Tablo 4. Changes in particle size of sludge

	Particle size (μm)				
	Surface-weighted average D [3.2]	Volume-weighted average D (4.3)	d (0.1)	d (0.5)	d (0.9)
Raw sludge	39	130	18.3	66.3	198
TiO_2/UV-A	30.1	76.5	17.4	57.2	152
TiO_2/UV-A/US	21.5	63.1	14.7	54.7	123.5
TiO_2/UV-B/Fe^{2+}	38.8	85.0	19.5	62.7	159
TiO_2/UV-B/Fe^0	37.7	95.5	18.7	61.4	164
TiO_2/UV-A/H_2O_2	20.1	73.2	13.8	63.8	145.4
TiO_2/UV-B/CFP	35.6	105	17.4	59.3	172
TiO_2/UV-B/Fe^0/US	28.5	82.2	14.2	75.8	160.4
TiO_2/UV-B/MFP	35.4	99.6	17.1	58.8	162
TiO_2/UV-B/MFP/US	17.9	52	10.5	41.3	105.5
TiO_2/UV-B/CFP/US	20	57.9	11.6	50.5	114.3
TiO_2/UV-A/H_2O_2/US	18.7	70.1	12	64.1	126.9
TiO_2/UV-B/Fe^{2+}/US	32.5	88.9	25	84.1	166.9

different oxidation processes. The results are shown in Fig. 9.

As shown in Fig. 9, after all the processes applied with ultrasound, the GP increased to 100%. This demonstrates that toxicity was significantly degraded after sludge disintegration by sono-photocatalytic processes. The cause of this increase is that persistent or complex organic/inorganic compounds become less toxic [41]. Ultrasonic treatment can deactivate the high organic load in the sludge, hence reducing the toxicity of this sludge [51,52].

9. Sludge Characterization

9-1. Particle Size Distribution

Particle size distribution analyses were performed for the sludge in the processes with the highest DD made. Thus, the effect of disintegration processes on sludge disintegration was determined. Particle size analysis was conducted in Sivas Cumhuriyet University Advanced Technology Research and Application Center (CÜTAM). Results are shown in Table 4. d (0.1), d (0.5), and d (0.9) describe 10, 50, and 90% of particles (in volume) having a diameter lower or equal to d (0.1), d (0.5), and d (0.9), respectively.

During the disintegration process, a considerable decrease takes place in the particle size in sludge due to deterioration of the floc structure caused by the forces applied to the sludge. The decrease in particle size enables the solids in the sludge to be hydrolyzed more easily due to the increased surface area generally associated with the reduction in particle volume [53]. In this study, particle size was reduced in all processes (Table 4) and the best result was obtained with TiO_2/UV-B/MFP/US. After disintegration, sludge amount decreased between 19.2% and 60% according to the volume-weighted average D [4.3]. Considering the amount of sludge coming out of treatment plants and disposal costs, these reduction rates provide a substantial advantage.

CONCLUSION

Sono-photocatalytic disintegration of sludge under various exper-

imental conditions was investigated. Synergistic effects under different UV lights were examined by using the sono-photocatalytic process and fenton reagents together. When TiO_2 and H_2O_2 were used together, as a result of photolysis of H_2O_2 by UV light, additional •OH was produced and this contributed to the increase of disintegration efficiency. When TiO_2 was used together with iron, DD values d ecreased due to the changes in surficial complexing properties. This situation was evident even in the presence of US. After disintegration, the sludge amount decreased between 19.2% and 60% according to the volume-weighted average D [4.3]. Sludge disintegration with sono-photocatalytic and sono-photocatalytic/Fenton processes will be an important alternative in the near future, where the importance of sludge minimization is increasing day by day. As a result of this study, it was determined that the Fenton reagents used with the sono-photocatalytic process have a highly effective synergistic effect on sludge disintegration. The results obtained from this study, which has not been done before, will be an important reference in the further disintegration studies as well as in the treatment studies.

ACKNOWLEDGEMENT

This work is supported by the Scientific Research Project Fund of Cumhuriyet University under the Project number M-776. The authors sincerely thank CÜBAP Chairmanship for their endorsement.

REFERANCES

1. Y. Liu, *Chemosphere*, **50**, 1 (2003).
2. H. Øegaard, *Water Sci. Technol.*, **49**, 31 (2004).
3. N. Nagao, T. Matsuyama, H. Yamamoto and T. Toda, *Process Biochem.*, **39**, 37 (2003).
4. F. Ye, H, Ji and Y. Ye, *J. Hazard. Mater.*, **219**, 164 (2012).
5. A. A. Babaei, M. Golshan and B. Kakavandi, *Process Saf. Environ. Prot.*, **149**, 35 (2021).
6. M. R. Al-Mamun, S. Kader, M. S. Islam and M. Z. H. Khan, *J. Environ. Chem. Eng.*, **7**, 103248 (2019).
7. M. Anjum, N. H. Al-Makishah and M. A. Barakat, *Process Saf. Environ. Prot.*, **102**, 615 (2016).
8. Y. Deng and J. D. Englehardt, *Water Res.*, **40**, 3683 (2006).
9. A. L. Linsebigler, G. Lu and J. T. Yates, *Chem. Rev.*, **95**, 735 (1995).
10. M. Stucchi, C. L. Bianchi, C. Argirusis, V. Pifferi, B. Neppolian, G. Cerrato and D. C. Boffito, *Ultrason. Sonochem.*, **40**, 282 (2018).
11. Q. Guo, C. Zhou, Z. Ma and X. Yang, *Adv. Mater.*, **31**, 1901997 (2019).
12. N. Jaafarzadeh, A. Takdastan, S. Jorfi, F. Ghanbari, M. Ahmadi and G. Barzegar, *J. Mol. Liq.*, **256**, 462 (2018).
13. M. S. Lucas and J. A. Peres, *Dyes Pigm.*, **71**, 236 (2006).
14. A. Gharaee, M. R. Khosravi-Nikou and B. Anvaripour, *J. Ind. Eng. Chem.*, **79**, 181 (2019).
15. P. Vaishnave, A. Kumar, R. Ameta, P. B. Punjabi and S. C. Ameta, *Arabian J. Chem.*, **7**, 981 (2014).
16. D. T. Sponza and R. Oztekin, *J. Chem. Eng. Process Tech.*, **4**, 147 (2013).
17. E. A. Serna-Galvis, A. M. Botero-Coy, D. Martínez-Pachón, A. Moncayo-Lasso, M., Ibáñez, F. Hernández and R. A. Torres-Palma, *Water Res.*, **154**, 349 (2019).
18. F. Ahmedchekkat, M. S. Medjram, M. Chiha and A. Mahmoud Ali Al-bsoul, *Chem. Eng. J.*, **178**, 244 (2011).
19. A. Al-Bsoul, M. Al-Shannag, M. Tawalbeh, A. A. Al-Taani, W. K. Lafi, A. Al-Othman and M. Alsheyab, *Sci. Total Environ.*, **700**, 134576 (2020).
20. D. Schieppati, F. Galli, M. L. Peyot, V. Yargeau, C. L. Bianchi and D. C. Boffito, *Ultrason. Sonochem.*, **54**, 302 (2019).
21. S. G. Babu, P. Karthik, M. C. John, S. K. Lakhera, M. Ashokkumar, J. Khim and B. Neppolian, *Ultrason. Sonochem.*, **50**, 218 (2019).
22. S. Yildiz and A. Olabi, *Waste and Biomass Valorization*, **1** (2021).
23. B. Bethi, S. H. Sonawane, G. S. Rohit, C. R. Holkar, D. V. Pinjari, B. A. Bhanvase and A. B. Pandit, *Ultrason. Sonochem.*, **28**, 150 (2016).
24. A. A. Isari, F. Hayati, B. Kakavandi, M. Rostami, M. Motevassel and E. Dehghanifard, *Chem. Eng. J.*, **392**, 123685 (2020).
25. M. Dükkancı, M. Vinatoru and T. J. Mason, *Ultrason. Sonochem.*, **21**, 846 (2014).
26. X. Sun, J. Liu, L. Ji, G. Wang, S. Zhao, J. Y. Yoon and S. Chen, *Sci. Total Environ.*, **737**, 139606 (2020).
27. X. Sun, W. You, X. Xuan, L. Ji, X. Xu, G. Wang, S. Zhao, G. Boczkaj, J. Y. Yoon and S. Chen, *Chem. Eng. J.*, 128600 (2021).
28. X. Sun, X. Xuan, Y. Song, X. Jia, L. Ji, S. Zhao, J. Y. Yoon, S. Chen, J. Liu and G. Wang, *Ultrason. Sonochem.*, **70**, 105311 (2021).
29. A. Davidsson and J. la Cour Jansen, *Vatten*, **62**, 335 (2006).
30. Q. Wang, M. Kuninobu, K. Kakimoto, H. I. Ogawa and Y. Kato, *Bioresour. Technol.*, **68**, 309 (1999).
31. D. Lu, K. Xiao, Y. Chen, Y. N. A. Soh and Y. Zhou, *Water Res.*, **142**, 138 (2018).
32. D. H. Kim, E. Jeong, S. E. Oh and H. S. Shin, *Water Res.*, **44**, 3093 (2010).
33. Y. Wang, Y. Pan, X. Li, K. Zhang and T. Zhu, *Water Environ. Res.*, **91**, 665 (2019).
34. X. Man, X. Ning, H. Zou, J. Liang, J. Sun, X. Lu and J. Sun, *Chemosphere*, **191**, 839 (2018).
35. C. Gong, J. Jiang and D. Li, *Sci. Total Environ.*, **532**, 495 (2015).
36. S. Yildiz and A. Cömert, *Int. J. Environ. Health Res.*, **30**, 89 (2020).
37. S. Yildiz and A. Olabi, *Chem. Eng. Technol.*, **44**, 95 (2021).
38. M. Kallel, C. Belaid, T. Mechichi, M. Ksibi and B. Elleuch, *Chem. Eng. J.*, **150**, 391 (2009).
39. B. Jin, S. Wang, L. Xing, B. Li and Y. Peng, *Bioresour. Technol.*, **200**, 587 (2016).
40. T. S. Chandra, S. N. Malik, G. Suvidha, M. L. Padmere, P. Shanmugam and S. N. Mudliar, *Bioresour. Technol.*, **158**, 135 (2014).
41. S. N. Malik, P. C. Ghosh, A. N. Vaidya, V. Waindeskar, S. Das and S. N. Mudliar, *Water Sci. Technol.*, **76**, 1001 (2017).
42. S. Parsons, *Advanced oxidation processes for water and wastewater treatment*, IWA Publishing: London, UK (2005).
43. F. Wang, S. Lu and M. Ji, *Ultrason. Sonochem.*, **13**, 334 (2006).
44. M. Oveisi, N. M. Mahmoodi and M. A. Asli, *J. Cleaner Production*, **222**, 669 (2019).
45. T. Wen, Y. Zhao, X. Jiao, G. Yang, Z. Zhang, W. Wang, T. Zhang, Q. Zhang and S. Song, *J. Cleaner Production*, **293**, 126184 (2021).
46. J. C. Kotz, P. M. Treichel and J. Townsend, *Chemistry and chemical reactivity*, Cengage Learning, Boston, USA (2012).
47. J. Arana, J. H. Melián, J. D. Rodríguez, O. G. Dıaz, A. Viera, J. P. Pena,

P. M. Marrero Sosa and V. E. Jiménez, *Catal. Today*, **76**, 279 (2002).
48. F. Bashiri, S. M. Khezri, R. R. Kalantary and B. Kakavandi, *J. Mol. Liq.*, **314**, 113608 (2020).
49. Y. Deng and R. Zhao, *Curr. Pollut. Rep.*, **1**, 167 (2015).
50. B. Kakavandi and M. Ahmadi, *Ultrason. Sonochem.*, **56**, 25 (2019).
51. T. F. Silva, R. Ferreira, P. A. Soares, D. R. Manenti, A. Fonseca, I. Saraiva, R. A. R. Boaventura and V. J. Vilar, *J. Environ. Manage.*, **164**, 32 (2015).
52. J. B. Welter, E. V. Soares, E. H. Rotta and D. Seibert, *J. Environ. Chem. Eng.*, **6**, 1390 (2018).
53. J. A. Müller, A. Winter and G. Strünkmann, *Water Sci. Technol.*, **49**, 97 (2004).